

Turbulence evolution in magnetized non-neutral plasmas

Abstract

The transverse dynamics of magnetized single-species plasmas confined in a Penning-Malmberg trap is analogous to that of an inviscid and incompressible two-dimensional (2D) fluid, and is characterized by phenomena like formation, filamentation and merger of vortex structures [1]. The turbulent relaxation of an electron plasma is investigated numerically with 2D particle-in-cell (PIC) simulations [2]. A multiresolution analysis based on 2D orthogonal wavelets is used to separate the coherent and incoherent parts of the flow and to investigate the dynamics and interplay of the two components [3]. Quantitative trends of the turbulence evolution are identified by computing probability density functions and structure functions of vorticity increments, and enstrophy spectra. This analysis highlights the influence of the initial conditions and fluctuations of the electron density on the late evolution of the system, possibly leading to configurations characterized by the persistence of coherent structures [3-6].

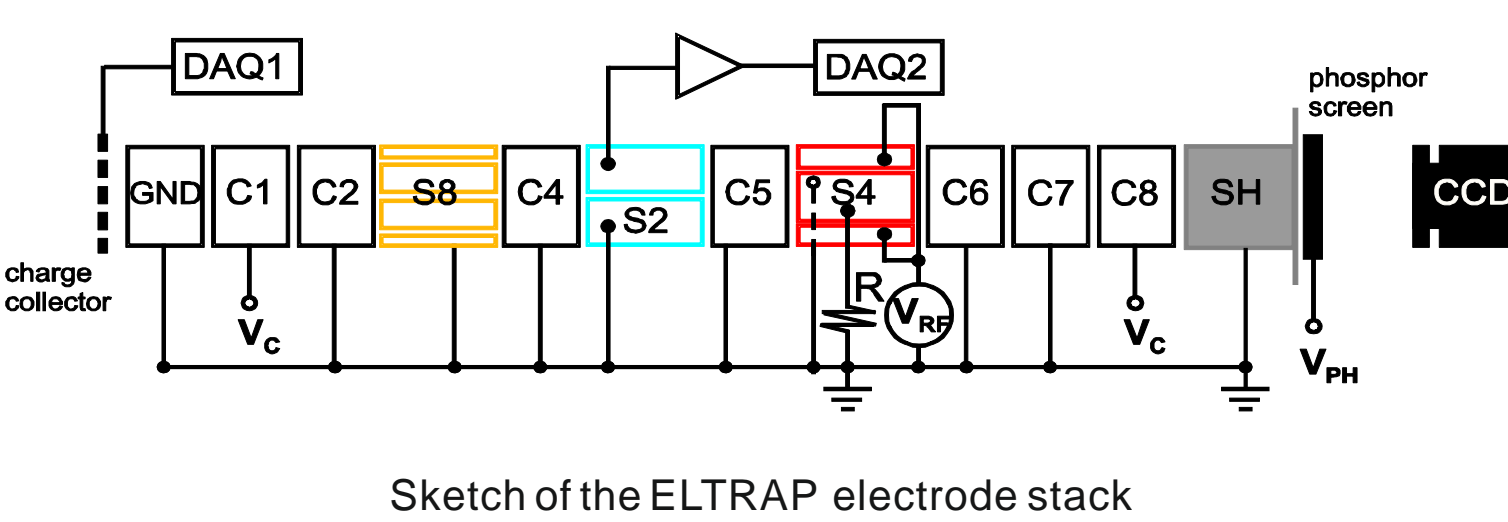
Non-neutral plasmas confined in Penning-Malmberg traps

A "non-neutral plasma" is a collection of unneutralized charges with linear dimensions $> \lambda_D$.

Non-neutral plasmas:

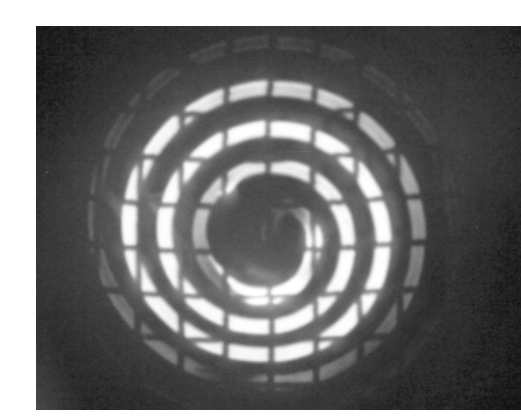
- can be confined by static electric and magnetic fields, and at the same time be in a state of thermal equilibrium (confined neutral plasmas can not be in a state of minimum free energy and instabilities can always be driven);
- allow quantitative tests of theory on fundamental plasma processes (equilibrium, transport, waves, control of instabilities);
- allow a test of fundamental fluid processes (vortex dynamics, turbulence evolution);
- find applications in many different fields as: charged particles beams; ultralow-uncertainty spectroscopy; antimatter production (e.g., Alpha, Atrap, Asacusa, Aegis experiments @ CERN).

Magnetized non-neutral plasmas can be confined for long times in Penning-Malmberg traps under UHV conditions ($p < 10^{-8}$ mbar) with a combination of static electric and magnetic fields, and their evolution can be monitored by means of electrostatic and optical systems.

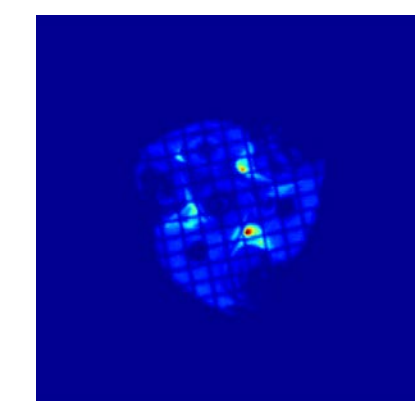


Plasma Generation

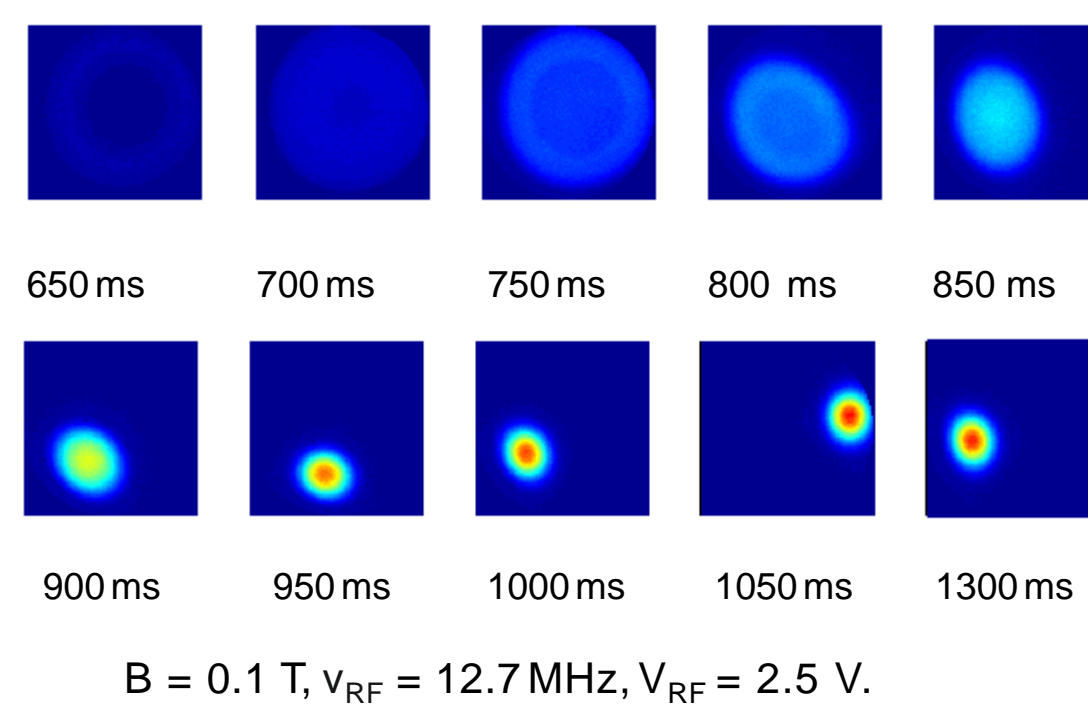
Thermionic emission



Field emission

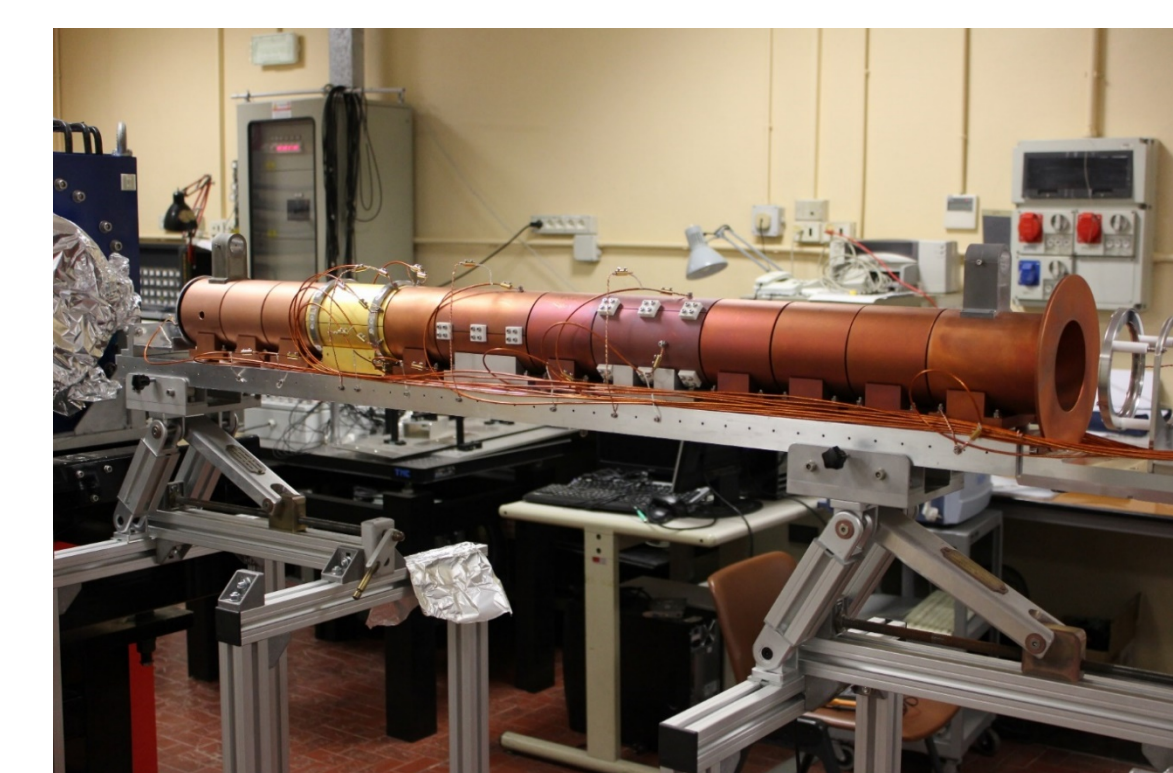


RF generation: $V_{RF} \sin(2\pi\nu_{RF}t)$ drive on one of the inner electrodes ($V_{RF} \sim 1-5$ V, $\nu_{RF} \sim 1-30$ MHz)



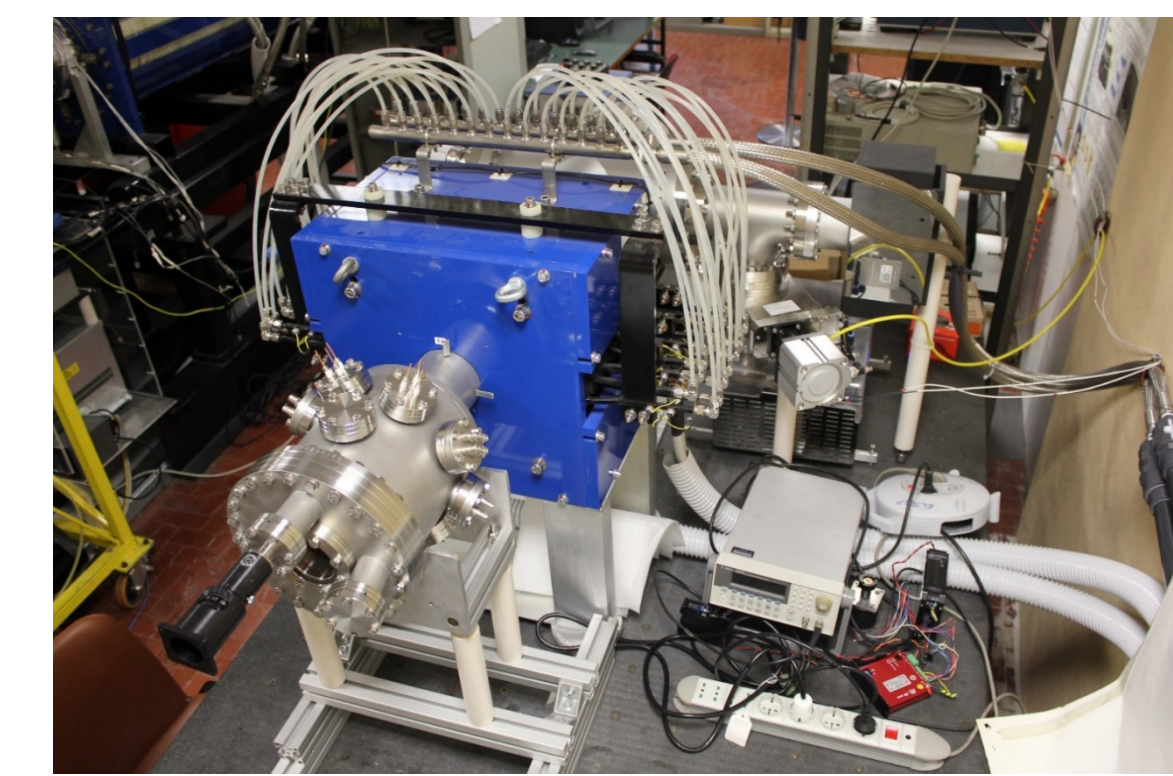
Penning-Malmberg traps @ Physics Department, Milano University

ELTRAP [7]



| Parameter | Range |
|--------------|--------------------------------|
| n_e | $10^6 - 10^8$ cm ⁻³ |
| B | ≤ 0.2 T |
| T_e | 1 - 10 eV |
| p | $10^{-9} - 10^{-8}$ mbar |
| $ V_{plug} $ | ≤ 100 V |
| L_p | 10 - 100 cm |
| R_w | 4.5 cm |

DUEL [8]

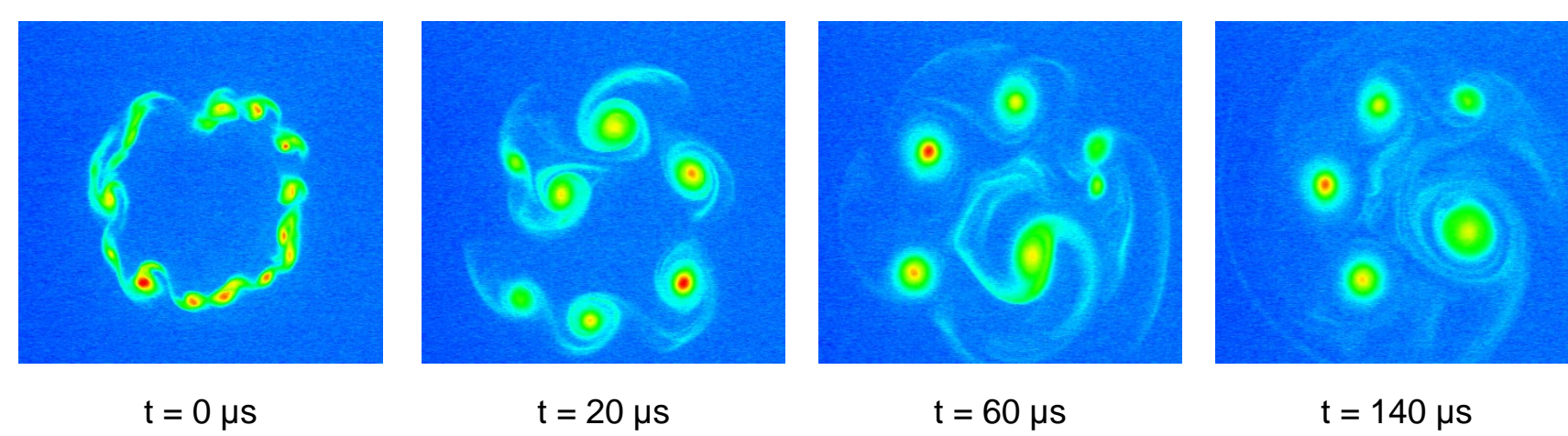


| Parameter | Range |
|--------------|--------------------------------|
| n_e | $10^6 - 10^8$ cm ⁻³ |
| B | ≤ 0.88 T |
| T_e | 1 - 10 eV |
| p | $10^{-9} - 10^{-8}$ mbar |
| $ V_{plug} $ | ≤ 200 V |
| L_p | 5 - 25 cm |
| R_w | 2.25 cm |

2D fluid dynamics experiments

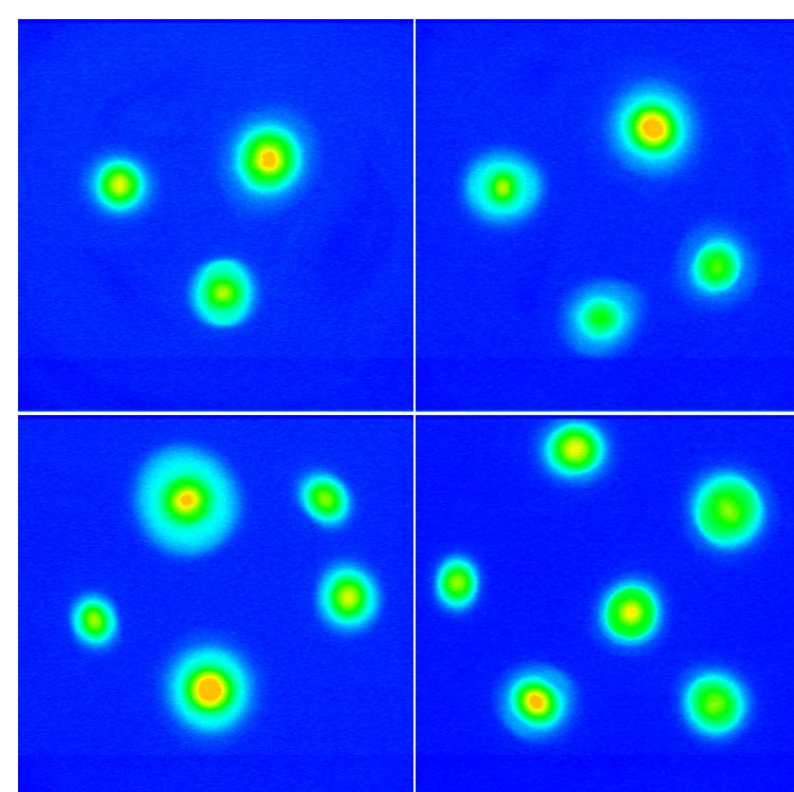
Electron plasmas allow to perform experiments on 2D fluid dynamics under almost ideal conditions (non-idealities are introduced by, e.g., inhomogeneities of the confining fields, finite resistivity of the wall, collisions with neutrals).

The evolution of the system can be reconstructed repeating several inject/hold/dump cycles with an increasing trapping time and with the same initial conditions. The evolution of the system is dominated by the diocotron (Kelvin-Helmholtz) instability due to the shear of the angular velocity, driving the plasma into a strongly non-linear regime in which vortex structures appear (eventually dissipated by viscosity effects on collisional time scales).



| 2D Ideal Fluid | 2D Electron Plasma |
|---|---|
| $\frac{\partial \zeta}{\partial t} + \mathbf{v} \cdot \nabla \zeta = 0$ | $\frac{\partial n}{\partial t} + \mathbf{v} \cdot \nabla n = 0$ |
| $\nabla^2 \psi = \zeta$ | $\nabla^2 \phi = 4\pi e n$ |
| $\mathbf{v} = \mathbf{e}_z \times \nabla \psi$ | $\mathbf{v} = \frac{\mathbf{e}_z \times \nabla \phi}{B}$ |
| $\zeta = (\nabla \times \mathbf{v}) \cdot \mathbf{e}_z$ | $\zeta = \frac{c}{B} \nabla^2 \phi = \frac{4\pi e c}{B} n$ |
| $\psi(\text{wall}) = \text{constant}$ | $\phi(\text{wall}) = \text{constant}$ |

The evolution of the system may lead to the formation of stable, rotating vortex patterns ("vortex crystals").



2D particle-in-cell simulations

$$\frac{\partial n}{\partial t} + \frac{1}{Br} \left(\frac{\partial \phi}{\partial t} \frac{\partial n}{\partial \theta} - \frac{\partial \phi}{\partial \theta} \frac{\partial n}{\partial r} \right) = 0, \quad \nabla^2 \phi = \frac{e}{\epsilon_0} n.$$

$$H \equiv -\frac{1}{2} \int d^2 \mathbf{r} n(\mathbf{r}, t) \phi(\mathbf{r}, t) = \text{const}, \quad L \equiv -\frac{1}{2} \int d^2 \mathbf{r} r^2 n(\mathbf{r}, t) = \text{const},$$

$$Z_j \equiv \frac{1}{j} \int d^2 \mathbf{r} n^j(\mathbf{r}, t) = \text{const} \quad (j \geq 1).$$

Initial density distributions:

- annular (the outer radius of the annulus is varied);
- spiral (the number of turns of the spiral is varied)

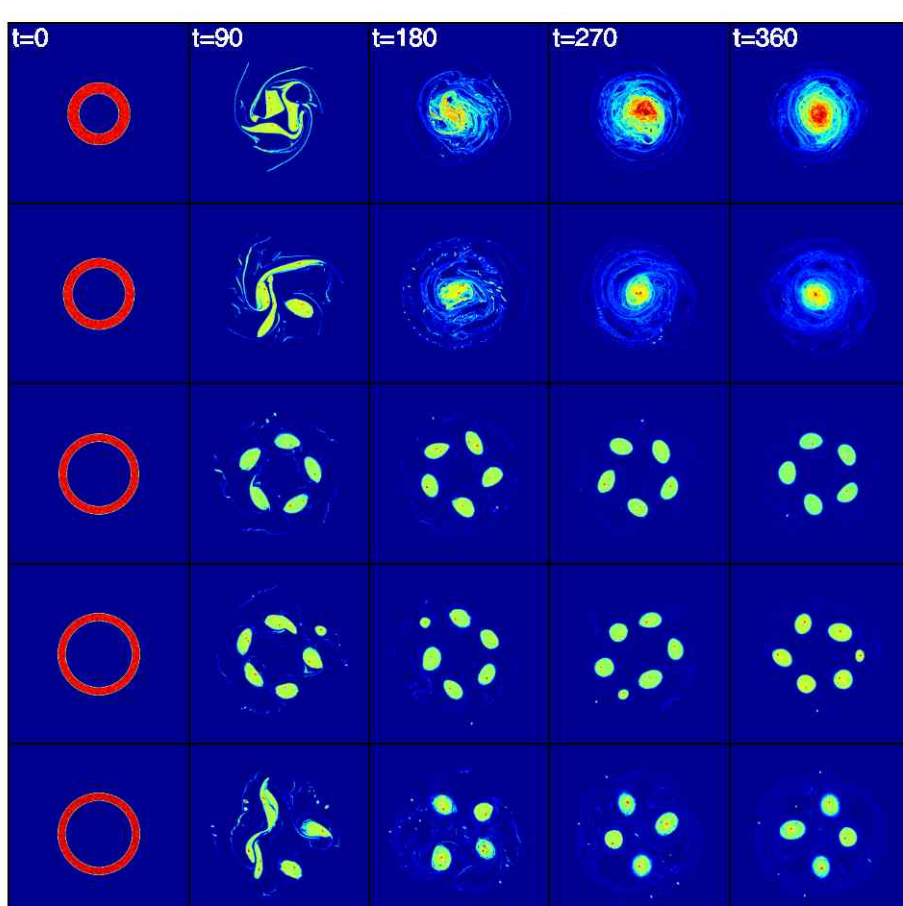
The initial area covered by the plasma is the same in all simulations.

$$n_0 = 10^7 \text{ cm}^{-3}; B = 1 \text{ T}; R_w = 2 \text{ cm}; t_f = 2 \text{ ms}; dt = 10^{-7} \text{ s}; N_{\text{macro}} = 10^6; 256 \times 256 \text{ grid}$$

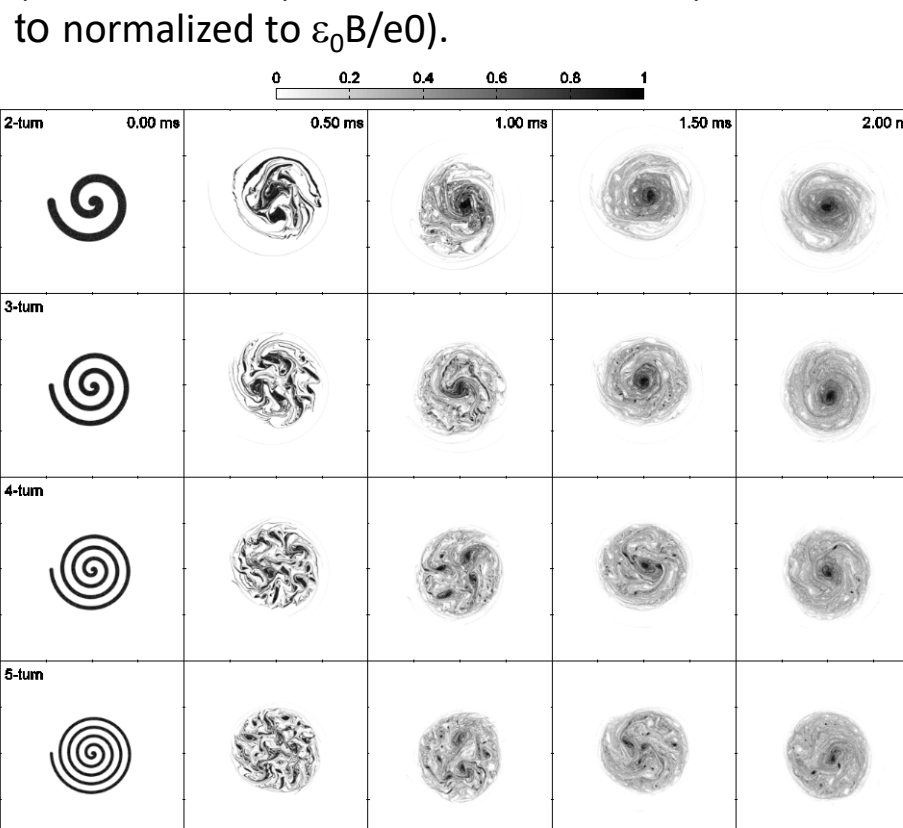
Experimentally, H and L are *robust* invariants, while Z_j ($j \geq 2$) are *fragile* or *dissipated* invariants. H and L are conserved in the PIC simulations with a relative accuracy of the order of 10^{-6} . The PIC method introduces an intrinsic effective "coarse-graining", which causes a non conservation of the topological invariants (with the obvious exception of Z_1).

Vortex dynamics and turbulence

Time evolution



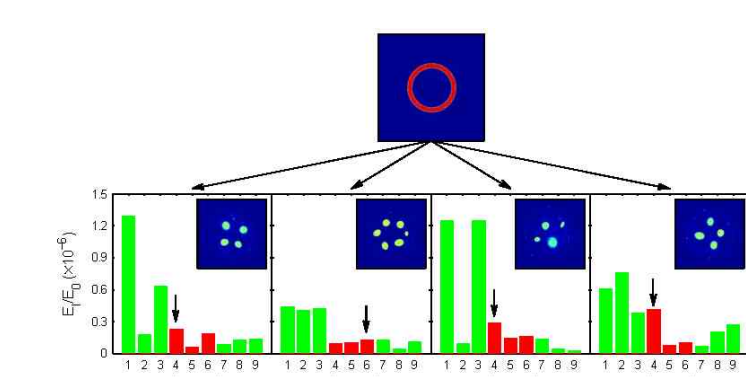
Annular density distributions with different outer radii: $r^*/R_w = 0.35, 0.40, 0.45$ and 0.46 (last two rows) and different times (normalized to normalized to $c_s B/e_0$).



For increasing N_{turns} : a) formation of a larger number of structures at increasingly smaller scales; b) faster evolution towards fully developed turbulence.

Effect of initial conditions and fluctuations

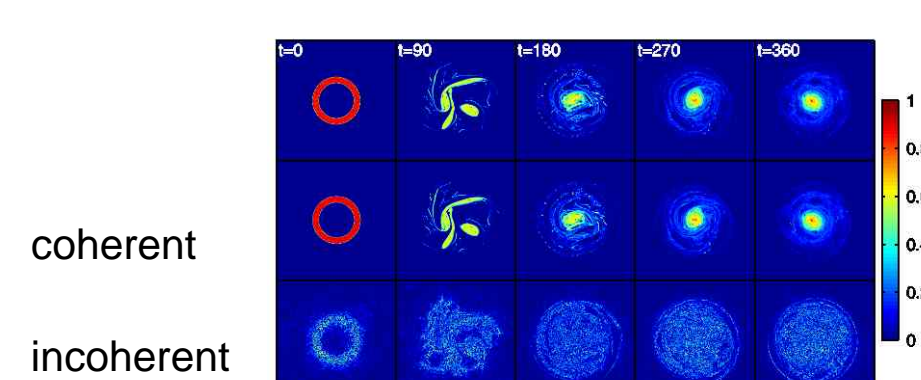
Fluctuations are introduced by the random number generator used to define the initial particle distribution. For annular configurations, crystalline states with different number of vortices are found due to slight variations of the initial energy content of different unstable diocotron modes with similar growth rates. In the experiments, fluctuations of the initial electron distribution may be due to, e.g., small changes of the source parameters or of the residual gas pressure.



Effect of initial fluctuations for a case where multiple competing (red bars) diocotron modes exist. The mode with the largest initial energy (arrow) survives in the final state (see insets).

Wavelet analysis

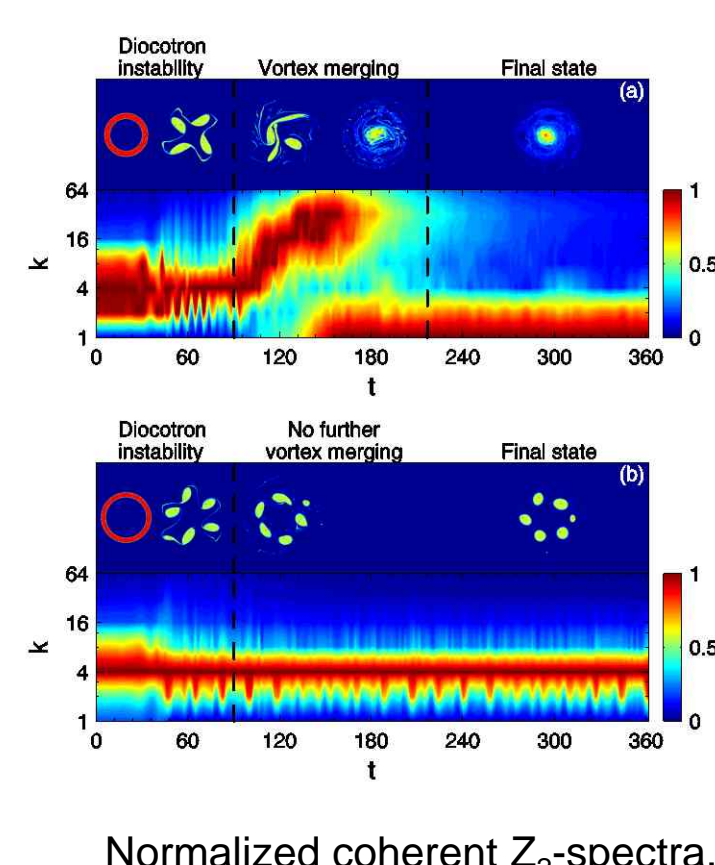
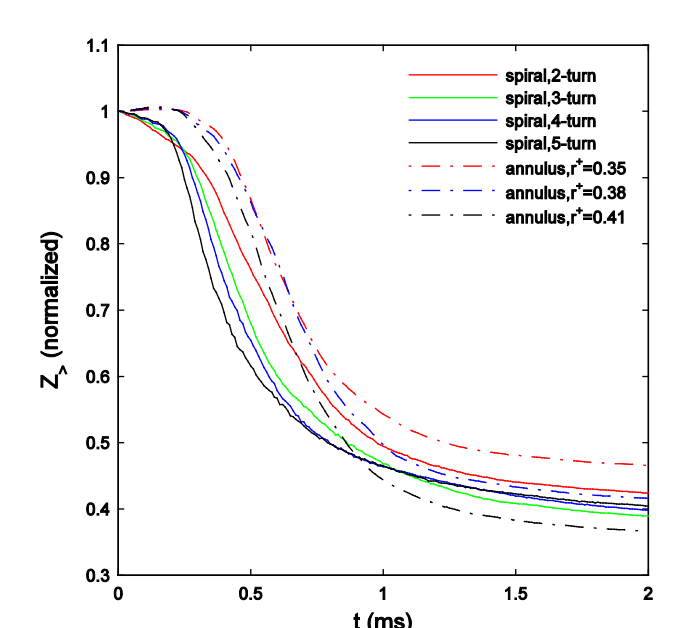
A characteristic feature of 2D turbulence is intermittency, defined as the presence of spatially localized bursts of small scale activity of a physical quantity (e.g., vorticity). Since intermittency is localized in both physical and spectral space, a suitable analysis tool for its study is the wavelet transform. A multi-resolution analysis is applied, which decomposes the vorticity field into coefficients containing coarse and fine details at increasing resolution. An adaptive self-consistent threshold is applied to separate the coherent and incoherent parts of the flow.



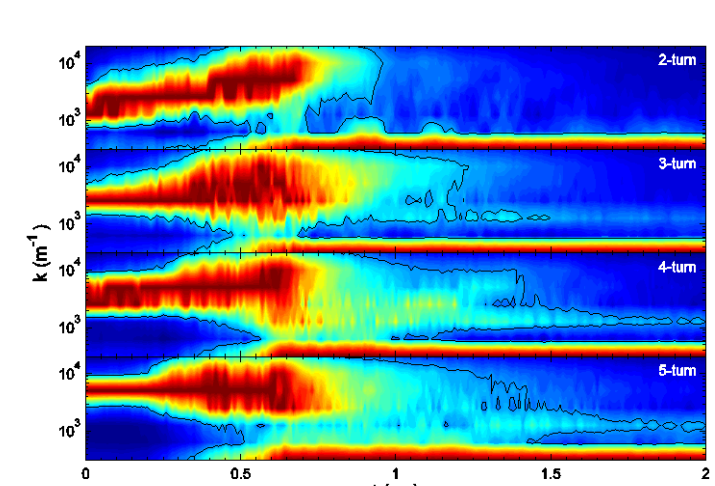
Only a small fraction ($< 2\%$) of the wavelet coefficients is necessary to represent the coherent component, which contains the greatest part ($> 95\%$) of Z_2 . The remaining small amplitude coefficients represent the incoherent component.

Enstrophy evolution

Enstrophy dissipation occurs mainly during merger events, as filaments of vorticity are stripped off the vortices. The filaments continue to elongate until their transverse spatial scale becomes smaller than a characteristic scale length (cell width in the case of the PIC simulations, Larmor radius scale in the real system), at which the enstrophy they contain is dissipated.



Normalized coherent Z_2 -spectra.



The vortex merging stage is related to the time interval in which the spectrum shows a "bifurcation" structure.

The instant at which the branch at larger k falls below a given value (e.g. half of the maximum value), is regarded as the time of turbulence development.

For spiral distributions, as N_{turns} increases the coherent Z_2 -spectrum shows that the vortex structures (formed at increasingly smaller scales) become more persistent, and it is again possible to estimate the time required to reach a state of fully developed turbulence.

References

- [1] M. Romé and F. Lepreti, Eur. Phys. J. Plus **126**, 38 (2011)
- [2] G. Maero, M. Romé, F. Lepreti, and M. Cavenago, Eur. Phys. J. D **68**, 277 (2014)
- [3] S. Chen, G. Maero, and M. Romé, J. Plasma Phys. **81**, 495810511 (2015)
- [4] M. Romé, S. Chen, and G. Maero, Plasma Sources Sci. Technol. **25**, 035016 (2016)

- [5] M. Romé, S. Chen, and G. Maero, Plasma Phys. Control. Fusion **59**, 014036 (2017)
- [6] S. Chen, G. Maero, and M. Romé, accepted for publication in J. Plasma Phys. (2017)
- [7] G. Maero, S. Chen, R. Pozzoli and M. Romé, J. Plasma Phys. **81**, 495810503 (2015)
- [8] M. Romé, F. Cavaliere, M. Cavenago, S. Chen, and G. Maero, AIP Conf. Proc. **1668**, 030001 (2015)